

Are your MRI contrast agents cost-effective?

Learn more about generic Gadolinium-Based Contrast Agents.



FRESENIUS  
KABI

caring for life

**AJNR**

**Anoxic Injury-Associated Cerebral  
Hyperperfusion Identified with Arterial  
Spin-Labeled MR Imaging**

J.M. Pollock, C.T. Whitlow, A.R. Deibler, H. Tan, J.H.  
Burdette, R.A. Kraft and J.A. Maldjian

This information is current as  
of April 20, 2024.

*AJNR Am J Neuroradiol* published online 1 May 2008  
<http://www.ajnr.org/content/early/2008/05/01/ajnr.A1095.citation>

ORIGINAL  
RESEARCH

J.M. Pollock  
C.T. Whitlow  
A.R. Deibler  
H. Tan  
J.H. Burdette  
R.A. Kraft  
J.A. Maldjian

# Anoxic Injury-Associated Cerebral Hyperperfusion Identified with Arterial Spin-Labeled MR Imaging

**BACKGROUND AND PURPOSE:** Anoxic brain injury is a devastating result of prolonged hypoxia. The goal of this study was to use arterial spin-labeling (ASL) to characterize the perfusion patterns encountered after anoxic injury to the brain.

**MATERIALS AND METHODS:** Sixteen patients with a history of anoxic or hypoxic-ischemic injury ranging in age from 1.5 to 78.0 years (mean, 50.3 years) were analyzed with conventional MR imaging and pulsed ASL 1.0–13.0 days (mean, 4.6 days) after anoxic insult. The cerebral perfusion in each case was quantified by using pulsed ASL as part of the standard stroke protocol. Correlation was made among perfusion imaging, conventional imaging, clinical history, laboratory values, and outcome.

**RESULTS:** Fifteen of the 16 patients showed marked global hyperperfusion, and 1 patient showed unilateral marked hyperperfusion. Mean gray matter (GM) cerebral blood flow (CBF) in these patients was 142.6 mL/100 g of tissue per minute (ranging from 79.9 to 204.4 mL/100 g of tissue per minute). Global GM CBF was significantly higher in anoxic injury subjects, compared with age-matched control groups with and without infarction ( $F_{2,39} = 63.11$ ;  $P < .001$ ). Three patients had global hyperperfusion sparing areas of acute infarction. Conventional imaging showed characteristic restricted diffusion in the basal ganglia ( $n = 10$ ) and cortex ( $n = 13$ ). Most patients examined died ( $n = 12$ ), with only 4 patients surviving at the 4-month follow-up.

**CONCLUSION:** Pulsed ASL can dramatically demonstrate and quantify the severity of the cerebral hyperperfusion after a global anoxic injury. The global hyperperfusion probably results from loss of autoregulation of cerebral vascular resistance.

Anoxic injuries resulting from global cessation of oxygenated cerebral blood flow (CBF) have profound effects on cerebral metabolism. Characteristic imaging findings include infarctions in regions with higher metabolic demands, including the basal ganglia and cerebral cortex.<sup>1–3</sup> Arterial spin-labeling (ASL) perfusion imaging generates qualitative and quantitative data. ASL perfusion imaging findings in these patients have not been described in the literature. Xenon CT perfusion has been used to evaluate postresuscitation patients with mixed results.<sup>4–6</sup> Other cerebral perfusion methods, such as nuclear medicine hexamethylpropyleneamine oxime single-photon emission CT and O-15 positron-emission tomography (PET), rely on differences in regional perfusion and may not detect a global symmetric hyperperfusion pattern.<sup>7</sup> The goal of this study was to use ASL to characterize the perfusion patterns encountered after anoxic injury to the brain. We present a series of 16 patients with a history of anoxic injury who demonstrated marked cerebral hyperperfusion on pulsed ASL perfusion imaging. We propose that this marked hyperperfusion is secondary to the loss of autoregulation of cerebral vascular resistance caused by the anoxic injury.

## Methods

Pulsed ASL was performed in 5000 consecutive clinical MR imaging examinations from December 2006 through January 2008. We retrospectively identified those patients with a discharge diagnosis or clinical history of hypoxic-ischemic or cerebral anoxic injury. Patient characteristics, including cerebral perfusion pattern, average gray matter (GM) CBF (in milliliters per 100 grams of tissue per minute), clinical history, laboratory data, and outcome were correlated with conventional imaging findings. The institutional review board at Wake Forest University approved this retrospective study.

Quantitative CBF maps were generated by using a Q2TIPS-FAIR sequence (second version of quantitative imaging of perfusion by using a single subtraction with addition of thin-section periodic saturation after inversion and a time delay sequence), as described previously.<sup>8</sup> Briefly, this sequence generates 60 tag and control image pairs. Imaging parameters are as follows: TE, 28 ms; TI, 1800 ms; TI<sub>1s</sub>, 1200 ms; TI, 2000 ms; TR, 3000 ms; receiver bandwidth, 62.5 kHz; flip angle, 90°; FOV, 24 cm (frequency) × 18 cm (phase), an acquisition matrix 64 × 48 (11 sections; 8-mm thickness; 0-mm section gap), and frequency encoding direction anterior/posterior. The sequence was performed by using Signa Excite HD scanners (GE Medical Systems, Milwaukee, Wis) at field strengths of 1.5T and 3T. A diffusion gradient with an equivalent b-value of 5.25 mm<sup>2</sup>/s is added to suppress intra-arterial spins.<sup>9</sup> Perfusion images were generated by using a fully automated data processing pipeline,<sup>10</sup> including data transfer to network attached storage, conversion from DICOM to Neuroimaging Informatics Technology Initiative format, motion correction, tissue segmentation, flow quantification, creation of color JPEG CBF maps, conversion back to DICOM format, and insertion into the clinical PACS. These steps are performed by using distributed grid processing with the Sun Grid Engine (Sun Microsystems, Santa Clara, Calif). The images are corrected for motion and then subtracted to generate the relative perfusion signal intensity maps. The perfusion maps are segmented with SPM5 (statistical parametric mapping)<sup>11</sup> based on the

Received November 30, 2007; accepted after revision February 6, 2008.

From the Department of Radiology (J.M.P., C.T.W., A.R.D., J.H.B., J.A.M.), Wake Forest University School of Medicine, Winston-Salem, NC; and Department of Biomedical Engineering (H.T., R.A.K.), Wake Forest University, Winston-Salem, NC.

This work was supported by the Human Brain Project and the National Institute of Biomedical Imaging and Bioengineering through grants EB004673 and EB004673-02S2. This work was also partially supported by the Center for Biomolecular Imaging of Wake Forest University School of Medicine.

Please address correspondence to Jeffrey M. Pollock, Wake Forest University School of Medicine, Department of Radiology, Medical Center Blvd, Winston-Salem, NC 27157; e-mail: jeffmpollock@gmail.com

DOI 10.3174/ajnr.A1095

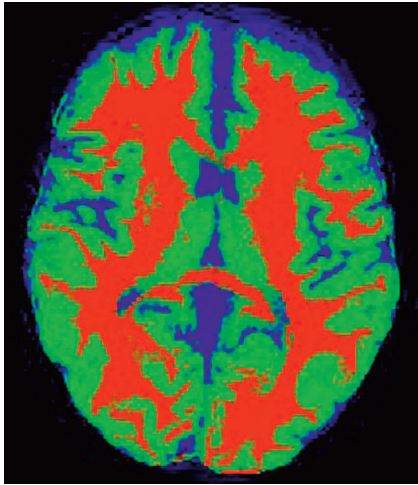


**Fig 1.** Segmentation map obtained by using the T1-weighted image shows CSF (blue), white matter (red), and GM (green). The green areas are used for the mean GM CBF measurements.

anatomic T1-weighted image (Fig 1) and then scaled by the mean signal intensity (M0) of blood. The segmentation and scaling step allows for voxel-wise computation of absolute CBF maps. The perfusion maps are colorized by using a standard scale, and a JPEG of the resulting image series is generated. The segmentation map is applied to the CBF data giving GM CBF quantification for the volume of acquisition, and the result is displayed on the JPEG image. Final gray-scale perfusion images and the colorized JPEG images are automatically converted back to DICOM format and sent to the PACS for systemwide review.

For comparative purposes, average GM perfusion values were also obtained from a retrospective analysis of 2 age- and sex-matched control groups. Group 1 included 13 patients with an indication of stroke with normal conventional and perfusion imaging. Group 2 included 14 patients with an indication of stroke with acute infarcts on diffusion imaging. A one-way analysis of covariance (ANCOVA) was performed by using pulsed ASL (PASL) measures of global CBF in GM as the dependent measure, group (infarction negative, infarction positive, and anoxic injury) as the independent variable, and age as a covariate.

## Results

The clinical features, laboratory values, and average GM perfusion values are listed in the Table. Sixteen patients (mean age, 50.3 years; range, 1.5–78.0 years) were identified with a history of anoxic injury. Nine patients had anoxic injuries outside of the hospital ( $n = 9$ ), and 7 patients had anoxic injuries inside the hospital ( $n = 7$ ). Only 5 patients had the duration of cardiopulmonary resuscitation documented (range, 30 seconds to 30 minutes). The average time between the anoxic episode and perfusion imaging was 4.6 days. Conventional imaging showed restricted diffusion in the basal ganglia in 10 patients and within the cortex in 13 patients (Fig 2). Partial pressure of carbon dioxide ( $\text{PCO}_2$ ) measurements obtained by arterial blood gas at the time of imaging averaged 38.6 mm Hg. Average GM CBF for the 16 patients was 142.6 mL/100 g of tissue per minute ( $\pm 36.2$  mL/100 g of tissue per minute), ranging from 79.9 to 204.4 mL/100 g of tissue per minute. Twelve patients showed marked symmetric global hyperperfusion ( $n = 12$ ; Fig 2). Three patients showed global hyperper-

fusion sparing previous areas of infarction ( $n = 3$ ; Fig 3A, -B). One patient showed unilateral hyperperfusion ( $n = 1$ ). Four patients survived, 1 remaining in a persistent vegetative state, 1 with severe encephalopathy, 1 with severe short-term memory loss, and 1 returning to baseline neurologic function. The patient who returned to baseline had the highest  $\text{PCO}_2$  measurement (54 mm Hg). The patients who survived had the least amount of diffusion abnormality. The remaining patients ( $n = 12$ ) died within 1 month of perfusion imaging.

Group 1 (infarction negative) had a mean  $\pm$  SD GM perfusion of  $68.3 \pm 10.9$  mL/100 g of tissue per minute. Group 2 (infarction positive) had a mean  $\pm$  SD GM perfusion of  $56.1 \pm 8.6$  mL/100 g of tissue per minute. Group 3 (anoxic injury) had a mean  $\pm$  SD GM perfusion of  $142.6 \pm 36.2$  mL/100 g of tissue per minute. For rates of global CBF in GM, ANCOVA revealed a main effect of group, such that rates of global CBF in GM were significantly different between groups ( $F_{2,39} = 63.11$ ;  $P < .001$ ). More specifically, Bonferroni-adjusted post hoc analyses of between-group differences revealed rates of CBF to be significantly higher in the anoxic injury group compared with the infarction-negative ( $P < .001$ ) and infarction-positive ( $P < .001$ ) groups (Fig 4). There was, however, no statistically significant difference in global rates of CBF between the infarction-positive and infarction-negative control groups ( $P = .12$ ).

## Discussion

ASL perfusion MR imaging was first described over a decade ago<sup>12,13</sup> and has been an active area of research.<sup>14,15</sup> One advantage of ASL over conventional bolus tracking for perfusion measurement is that it provides absolute CBF information. Quantification of CBF facilitates the identification of cases with symmetric global perfusion abnormalities (Fig 2).

Causes of global cerebral hyperperfusion include etiologies that result in global vasodilation or loss of cerebral vascular autoregulation. Carbon dioxide is a potent vasodilator, and hypercapnia can cause transient vasodilation when cerebral perfusion autoregulation pathways are intact.<sup>16-19</sup> This property has been exploited with tests, such as the hypercapnia challenge, to evaluate the cerebral vascular reserve.<sup>17</sup> All of the patients in our series had normal arterial blood gas measurements except for case 6. Case 6 is a case of favorable outcome while showing global hyperperfusion. Previous studies have shown up to a 200% increase in CBF as  $\text{PCO}_2$  increases to values similar to case 6 ( $\text{PCO}_2$ , 54).<sup>18-26</sup> We believe that the global hyperperfusion in case 6 is a result of hypercapnia rather than anoxia.

Autoregulation of cerebral perfusion has been an active area of research.<sup>17,18,20,27-29</sup> Autoregulation of CBF maintains the relationship  $\text{CBF} = \text{CPP}/\text{CVR}$ , where CPP is cerebral perfusion pressure and CVR is cerebral vascular resistance. As long as the cerebral arterioles can constrict and dilate to modulate CVR, they can accommodate a range of cerebral perfusion pressures and maintain constant CBF. When autoregulation is absent, CVR remains constant, and CBF is proportional to CPP, which is defined as mean arterial pressure minus intracranial pressure. Thus, when autoregulation is lost, CBF is proportional to mean arterial pressure.<sup>27-29</sup>

Several pathways have been hypothesized to account for autoregulation, including the myogenic response, neurogenic

**Clinical and imaging findings in 16 patients with anoxic injury**

Patient/ Sex	Age, y	Etiology of Anoxic Event	Event Location and Duration	Interval between Event and Imaging, days	Pco <sub>2</sub> , mm Hg	Diffusion Restriction Location	Average GM CBF, mL/100 g/min	Hyperperfusion Pattern	Outcome
1/M	56	Hypoglycemia	Out, unknown	2	40.8	BG, diffuse cortex	93.5	Unilateral	Died
2/M	11	Septic Shock	In, unknown	9	32.9	BG, diffuse cortex	190.6	Global	Died
3/F	56	Cardiac arrest	In, 3 minutes	7	35.4	BG, posterior watershed	79.9	Global, sparing infarct	Died
4/M	31	Electroconvulsion	Out, unknown	2	39.7	BG, posterior watershed	140.3	Global	Persistent Vegetative
5/F	69	PEA	Out, unknown	2	42.9	BG, diffuse watershed	144.9	Global	Died
6/F	46	Cardiac arrest	Out, unknown	6	54	BG	101.7	Global	Survived
7/M	75	Cardiac arrest	In, unknown	3	33.6	BG, periventricular	142.7	Global	Died
8/F	37	PEA	In, 30 seconds	3	26.8	Left MCA, bilateral PCA	125.8	Global, sparing infarct	Died
9/F	71	Cardiac arrest	Out, unknown	2	37.1	Bilateral PCA	107.8	Global, sparing infarct	Died
10/M	44	Septic shock	Out, unknown	13	36.9	Mild diffuse cortical	146.1	Global	Died
11/F	51	Cardiac arrest	In, 30 minutes	6	43.2	BG, diffuse cortex	126.2	Global	Died
12/F	64	Cardiac arrest	Out, unknown	1	45.4	Mild diffuse cortical	188.1	Global	Died
13/F	1.5	Seizure	Out, 7 minutes	3	37.9	BG, white matter, cortical	204.4	Global	Died
14/M	59	Cardiac arrest	In, unknown	5	37.3	BG, posterior watershed	177.5	Global	Died
15/F	78	Cardiac arrest	In, 10 minutes	1	34.9	None	161.7	Global	Encephalopathy
16/F	56	Cardiac arrest	Out, unknown	6	39.0	None	150.7	Global	Short-term memory loss
Average	50.3			4.6 days	38.6		142.6		

**Note:**—PEA indicates pulseless electrical activity; In, in hospital; Out, outside hospital; BG, basal ganglia; MCA, middle cerebral artery; PCA, posterior cerebral artery; Pco<sub>2</sub>, partial pressure of carbon dioxide.

response, and the metabolic response, including the metabolites CO<sub>2</sub>, adenosine, potassium, nitric oxide, and calcium.<sup>17,27,28</sup> Little human research exists regarding the effect of global anoxia on autoregulation.<sup>4,20,29-37</sup> Animal models have shown a loss of cerebral vascular resistance in the postanoxic state resulting in uncontrolled hyperperfusion.<sup>38-42</sup> Cerebral blood volume has been shown to increase with loss of autoregulation secondary to ischemia, but no large studies have demonstrated a similar relationship for CBF.<sup>43</sup> Relative hyperperfusion has been shown in the thalamus, cerebellum, and occipital lobes with O-15 PET imaging in resuscitated patients; however, this method does not quantitate flow.<sup>36</sup> Schaafsma et al<sup>36</sup> believed this hyperperfusion was secondary to a “postanoxic disturbance of autoregulation.” We believe that a similar loss of autoregulation accounts for the cerebral hyperperfusion seen in our ASL patient series.<sup>20,36,38</sup>

Xenon-CT perfusion has been used to evaluate CBF after cardiac resuscitation. A study by Cohan et al<sup>4</sup> showed an increase in global whole-brain CBF by up to 300% in nonsurviving patients. The CBF values obtained in the 6 patients who died in the Cohan et al study closely parallel the mean and range of our ASL data. Cohan et al showed, by using the fast flow compartment method, that the nonsurviving group mean cerebral perfusion was 145 mL/100 g of tissue per minute, ranging from 110 to 190 mL/100 g of tissue per minute.

A similar but less dramatic increase in cerebral perfusion was shown by Inoue et al<sup>5</sup> by using serial xenon-CT perfusion studies during the week after the ischemic event. However, the values for CBF were significantly lower than the study by Cohan et al<sup>4</sup> and were only hyperperfused relative to controls in patients who survived.<sup>5</sup> A study by Nogami et al<sup>6</sup> using xenon-CT perfusion 8–20 days after the hypoxic event showed a decrease in hemispheric CBF in patients with a severe disability, but also noted hyperperfusion within the putamen. This study was based on region-of-interest placement rather than global GM quantification. Given that several of the patients had cortical and laminar necrosis, there may have been an artificially decreased perfusion measurement if an area of infarction was selected for the region of interest.

The discrepancies between the xenon-based studies are probably multifactorial. Different methodologies, different time periods, (initial 48 hours, initial week, and from 8 to 20 days), technical factors, exclusion of nonsurvivors in 2 studies, small sample size of nonsurvivors (*n* = 6, Cohan et al<sup>4</sup>), and persistent vegetative state (*n* = 2, Inoue et al<sup>5</sup>, and *n* = 8, Nogami et al<sup>6</sup>) make it difficult to draw conclusions regarding the discrepancies between the xenon perfusion studies and the ASL data. Comparing the quantitative perfusion values between xenon and ASL is inconclusive, because 2 of the xenon-based studies used hemispheric perfusion values, whereas our ASL data were limited to GM perfusion. The xenon perfusion values and poor clinical outcomes (death) reported by Cohan et al<sup>4</sup> most closely resemble our data with ASL.

Age has been shown to greatly affect cerebral perfusion, peaking at age 5–8 years.<sup>44,45</sup> The quantitative nature of ASL allowed us to show that the 2 youngest patients in our series (1.5 and 11.0 years old) showed the highest average cerebral perfusion. We believe that normal age-related changes compounded the global hyperperfusion associated with the anoxic injury.

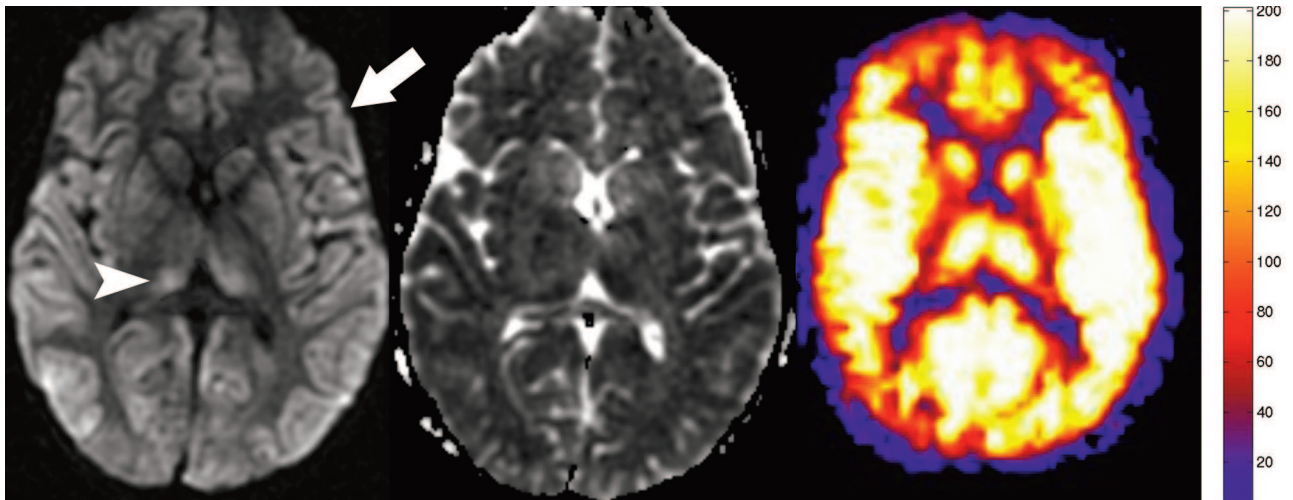


**Fig 2.** Axial diffusion-weighted, apparent diffusion coefficient (ADC), and quantitative CBF map from patient 2 shows the typical sequelae from anoxic injury, including diffuse bilateral symmetric restricted diffusion in the cerebral cortex (*arrow*) and the basal ganglia and thalami (*arrowhead*). The ADC image reflects the subacute nature of the ischemic change, because the imaging was done 9 days after the anoxic event. CBF map shows global hyperperfusion and the second highest average GM blood flow recorded in this study (190.6 mL/100 g of tissue per minute).

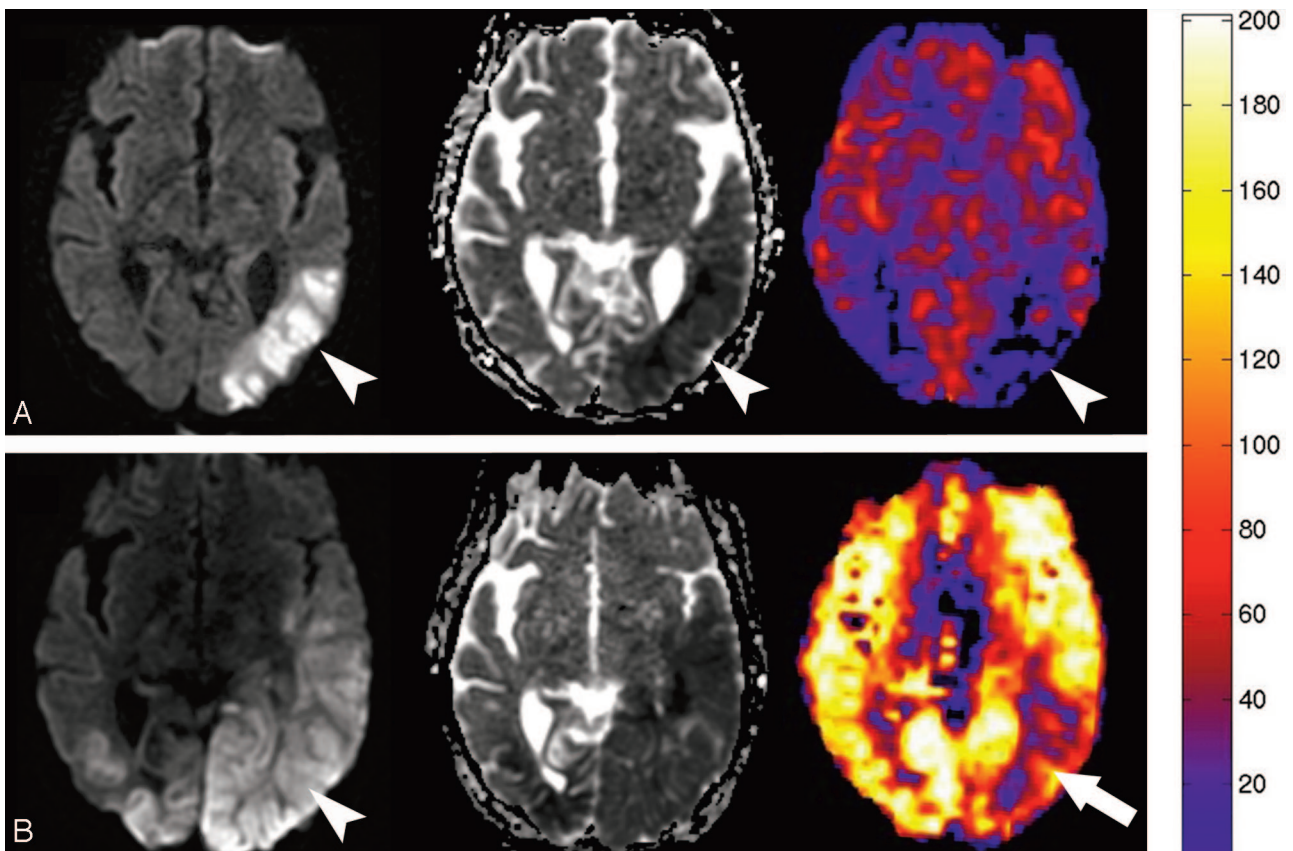


**Fig 3.** A, Diffusion, ADC, and quantitative CBF map generated from the PASL sequence obtained in patient 8 one day before the global anoxic event shows restricted diffusion and hypoperfusion in the left posterior watershed territory corresponding with areas of subacute infarction (*arrowheads*). B, Diffusion, ADC, and quantitative CBF map obtained 3 days after the episode of pulseless electrical activity in patient 8 shows interval worsening of the diffusion abnormality (*arrowhead*) with new marked global hyperperfusion. There is relative sparing of the previous subacute infarct in the left posterior MCA territory (*arrow*). Quantitative analysis performed by placing regions of interest over the entire section showed an average CBF increase from 31.4 to 188.6 mL/100 g of tissue per minute.

When a pattern of global cerebral perfusion is encountered in clinical practice, the radiologist should correlate the perfusion values with the patient's age, arterial blood gas measurements, conventional imaging, and clinical history. When the patient demonstrates global superphysiologic perfusion val-

ues, has no evidence of hypercapnia, and conventional diffusion imaging shows early associated infarctions of the basal ganglia and cortex,<sup>1</sup> global cerebral anoxic injury should be strongly considered in the differential diagnosis.

It is unclear whether the global cerebral hyperperfusion

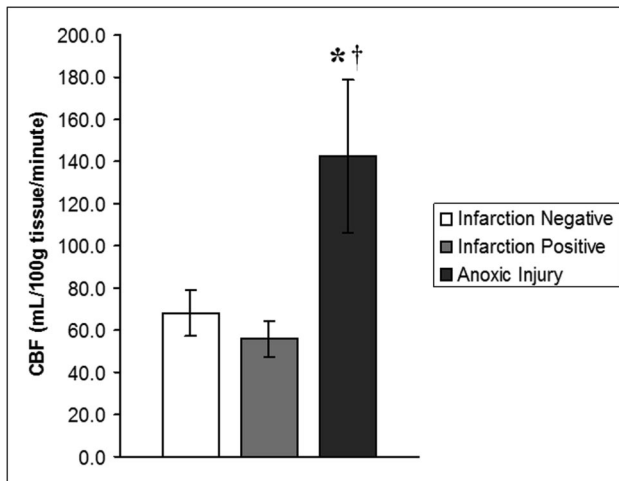


**Fig 4.** Graph demonstrates rates of global GM CBF (in milliliters per 100 grams per minute), expressed as means  $\pm$  SDs for 3 groups (infarction negative, infarction positive, and anoxic injury). Rates of global CBF in the anoxic injury group are 109% and 154% higher than rates of CBF in the infarction-negative and infarction-positive control groups, respectively. Data show a statistically significant difference between the anoxic injury and infarction-negative (\*) groups and infarction-positive (†) groups. There was no statistically significant difference in global rates of CBF between the infarction-positive and infarction-negative groups.

pattern causes further microvascular damage or whether it serves some potential benefit. It is equally unclear whether pharmacologic regulation of this hyperperfusion through strict control of mean arterial blood pressure could have any significant benefit to the patient. With 12 of 16 normocapnic patients in our series dying within 4 weeks of perfusion imaging, it is clear that the natural course of anoxic-related cerebral injuries is devastating.<sup>2,35,36</sup> Of the patients who survived in our series ( $n = 4$ ), 1 patient was probably hypercapnic and returned to baseline function. The remaining survivors had unfavorable outcomes, including persistent vegetative state, severe encephalopathy, and profound short-term memory difficulties similar to those reported previously.<sup>36</sup>

Future trials with animal models may elucidate treatment strategies to preserve function and improve outcome. Recent animal models and clinical studies of global ischemia have shown promising neuroprotective effects of mild-to-moderate therapeutic hypothermia.<sup>46-49</sup> Future potential studies with ASL may examine the effects of hypothermia and other treatment strategies on cerebral perfusion in the anoxic patient.

## Conclusion

Global cerebral hyperperfusion secondary to irrecoverable loss of vascular resistance will be increasingly recognized as perfusion imaging is more widely clinically implemented. When global cerebral hyperperfusion is encountered, the short list of diagnostic considerations includes a normal young patient, hypercapnia, and anoxic injury. Correlation with conventional imaging, laboratory values, and clinical history should distinguish these entities. Currently the finding of global hyperperfusion associated with anoxic injury is an ominous sign and portends a poor outcome.<sup>2,4,20,50</sup> The superphysiologic perfusion shown on ASL may open a door to further research opportunities aimed to improve outcome and establish treatment guidelines for global anoxic injuries.<sup>51</sup>

## Acknowledgments

We thank Kathy Pearson for help with computer programming. We also thank Becky J. Mussat-Whitlow for reviewing the statistical data.

## References

- Arbelaez A, Castillo M, Mukherji SK. Diffusion-weighted MR imaging of global cerebral anoxia. *AJNR Am J Neuroradiol* 1999;20:999-1007
- McKinney AM, Teksam M, Felice R, et al. Diffusion-weighted imaging in the setting of diffuse cortical laminar necrosis and hypoxic-ischemic encephalopathy. *AJNR Am J Neuroradiol* 2004;25:1659-65
- Tha KK, Terae S, Yamamoto T, et al. Early detection of global cerebral anoxia: improved accuracy by high-b-value diffusion-weighted imaging with long echo time. *AJNR Am J Neuroradiol* 2005;26:1487-97
- Cohan SL, Mun SK, Petite J, et al. Cerebral blood flow in humans following resuscitation from cardiac arrest. *Stroke* 1989;20:761-65
- Inoue Y, Shiozaki T, Irisawa T, et al. Acute cerebral blood flow variations after human cardiac arrest assessed by stable xenon enhanced computed tomography. *Curr Neurovasc Res* 2007;4:49-54
- Nogami K, Fujii M, Kato S, et al. Analysis of magnetic resonance imaging (MRI) morphometry and cerebral blood flow in patients with hypoxic-ischemic encephalopathy. *J Clin Neurosci* 2004;11:376-80
- Giubilei F, Lenzi GL, Di Piero V, et al. Predictive value of brain perfusion single-photon emission computed tomography in acute ischemic stroke. *Stroke* 1990;21:895-900
- Luh WM, Wong EC, Bandettini PA, et al. QUIPSS II with thin-slice T1 periodic saturation: a method for improving accuracy of quantitative perfusion imaging using pulsed arterial spin labeling. *Magn Reson Med* 1999;41:1246-54
- Yang Y, Frank JA, Hou L, et al. Multislice imaging of quantitative cerebral perfusion with pulsed arterial spin labeling. *Magn Reson Med* 1998;39:825-32
- Maldjian J, Laurienti P, Burdette J, et al. Clinical implementation of spin tag perfusion MRI. *J Comput Assist Tomogr* 2008. In press.
- Friston KJ, Holmes AP, Worsley KJ, et al. Statistical parametric maps in functional imaging: a general linear approach. *Hum Brain Mapp* 1995;2:189-202
- Detre JA, Leigh JS, Williams DS, et al. Perfusion imaging. *Magn Reson Med* 1992;23:37-45
- Detre JA, Williams DS, Koretsky AP. Nuclear magnetic resonance determination of flow, lactate, and phosphate metabolites during amphetamine stimulation of the rat brain. *NMR Biomed* 1990;3:272-78
- Alsop DC, Detre JA. Multisection cerebral blood flow MR imaging with continuous arterial spin labeling. *Radiology* 1998;208:410-16
- Wong EC, Buxton RB, Frank LR. Quantitative perfusion imaging using arterial spin labeling. *Neuroimaging Clin N Am* 1999;9:333-42
- Busija DW, Heistad DD. Factors involved in the physiological regulation of the cerebral circulation. *Rev Physiol Biochem Pharmacol* 1984;101:161-211
- Faraci FM, Breese KR, Heistad DD. Cerebral vasodilation during hypercapnia. Role of glibenclamide-sensitive potassium channels and nitric oxide. *Stroke* 1994;25:1679-83
- Madden JA. The effect of carbon dioxide on cerebral arteries. *Pharmacol Ther* 1993;59:229-50
- Claassen JA, Zhang R, Fu Q, et al. Transcranial Doppler estimation of cerebral blood flow and cerebrovascular conductance during modified rebreathing. *J Appl Physiol* 2007;102:870-77
- Hanigan WC, Aldag J, Sabo RA, et al. Strangulation injuries in children. Part 2. Cerebrovascular hemodynamics. *J Trauma* 1996;40:73-77
- Koons A, Hegyi T, Mehta R, et al. Cerebral vascular responses to changes in carbon dioxide tension in term and preterm infants with apnea. *Biol Neonate* 2003;84:115-18
- Kastrup A, Li TQ, Glover GH, et al. Cerebral blood flow-related signal changes during breath-holding. *AJNR Am J Neuroradiol* 1999;20:1233-38
- Vovk A, Cunningham DA, Kowalchuk JM, et al. Cerebral blood flow responses to changes in oxygen and carbon dioxide in humans. *Can J Physiol Pharmacol* 2002;80:819-27
- Ito H, Kanno I, Ibaraki M, et al. Effect of aging on cerebral vascular response to PaCO<sub>2</sub> changes in humans as measured by positron emission tomography. *J Cereb Blood Flow Metab* 2002;22:997-1003
- Noth U, Kotajima F, Deichmann R, et al. Mapping of the cerebral vascular response to hypoxia and hypercapnia using quantitative perfusion MRI at 3 T. *NMR Biomed*. 2007 Sep 13 [Epub ahead of print]
- Noth U, Meadows GE, Kotajima F, et al. Cerebral vascular response to hypercapnia: determination with perfusion MRI at 1.5 and 3.0 Tesla using a pulsed arterial spin labeling technique. *J Magn Reson Imaging* 2006;24:1229-35
- Paulson OB, Strandgaard S, Edvinsson L. Cerebral autoregulation. *Cerebrovasc Brain Metab Rev* 1990;2:161-92
- Mathew RJ. Postural syncope and autoregulation of cerebral blood flow. *Biol Psychiatry* 1996;40:923-26

29. Sundgreen C, Larsen FS, Herzog TM, et al. **Autoregulation of cerebral blood flow in patients resuscitated from cardiac arrest.** *Stroke* 2001;32:128–32
30. Lillywhite N, Matta B. **Loss of cerebral pressure autoregulation and vasoreactivity to carbon dioxide after cerebral hypoxia.** *Anaesth Intensive Care* 1996;24:91–93
31. Nishizawa H, Kudoh I. **Cerebral autoregulation is impaired in patients resuscitated after cardiac arrest.** *Acta Anaesthesiol Scand* 1996;40:1149–53
32. Immink RV, van den Born BJ, van Montfrans GA, et al. **Impaired cerebral autoregulation in patients with malignant hypertension.** *Circulation* 2004;110:2241–45
33. Cruz J, Jaggi JL, Hoffstad OJ. **Cerebral blood flow, vascular resistance, and oxygen metabolism in acute brain trauma: redefining the role of cerebral perfusion pressure?** *Crit Care Med* 1995;23:1412–17
34. Agnoli A, Fieschi C, Bozzao L, et al. **Autoregulation of cerebral blood flow. Studies during drug-induced hypertension in normal subjects and in patients with cerebral vascular diseases.** *Circulation* 1968;38:800–12
35. Gueugniaud PY, Garcia-Darennes F, Gaussorgues P, et al. **Prognostic significance of early intracranial and cerebral perfusion pressures in post-cardiac arrest anoxic coma.** *Intensive Care Med* 1991;17:392–98
36. Schaafsma A, de Jong BM, Bams JL, et al. **Cerebral perfusion and metabolism in resuscitated patients with severe post-hypoxic encephalopathy.** *J Neurol Sci* 2003;210:23–30
37. Deibler A, Pollock JM, Kraft R, et al. **M. Arterial spin-labeling in routine clinical practice part 3: hypoperfusion patterns.** *AJNR Am J Neuroradiol*. 2008 Mar 20 [Epub ahead of print]
38. Panerai RB. **Assessment of cerebral pressure autoregulation in humans—a review of measurement methods.** *Physiol Meas* 1998;19:305–38
39. Bickler PE. **Cerebral anoxia tolerance in turtles: regulation of intracellular calcium and pH.** *Am J Physiol* 1992;263:R1298–302
40. Bickler PE. **Effects of temperature and anoxia on regional cerebral blood flow in turtles.** *Am J Physiol* 1992;262:R538–41
41. Mortberg E, Cumming P, Wiklund L, et al. **A PET study of regional cerebral blood flow after experimental cardiopulmonary resuscitation.** *Resuscitation* 2007;75:98–104
42. Laudignon N, Farri E, Beharry K, et al. **Influence of adenosine on cerebral blood flow during hypoxic hypoxia in the newborn piglet.** *J Appl Physiol* 1990;68:1534–41
43. Paulson OB, Lassen NA, Skinhoj E. **Regional cerebral blood flow in apoplexy without arterial occlusion.** *Neurology* 1970;20:125–38
44. Wang J, Licht DJ, Jahng GH, et al. **Pediatric perfusion imaging using pulsed arterial spin labeling.** *J Magn Reson Imaging* 2003;18:404–13
45. Wintermark M, Lepori D, Cotting J, et al. **Brain perfusion in children: evolution with age assessed by quantitative perfusion computed tomography.** *Pediatrics* 2004;113:1642–52
46. Hoesch RE, Geocadin RG. **Therapeutic hypothermia for global and focal ischemic brain injury—a cool way to improve neurologic outcomes.** *Neurologist* 2007;13:331–42
47. Agnew DM, Koehler RC, Guerguerian AM, et al. **Hypothermia for 24 hours after asphyxial cardiac arrest in piglets provides striatal neuroprotection that is sustained 10 days after rewarming.** *Pediatr Res* 2003;54:253–62
48. Shaffner DH, Eleff SM, Koehler RC, et al. **Effect of the no-flow interval and hypothermia on cerebral blood flow and metabolism during cardiopulmonary resuscitation in dogs.** *Stroke* 1998;29:2607–15
49. Rutherford MA, Azzopardi D, Whitelaw A, et al. **Mild hypothermia and the distribution of cerebral lesions in neonates with hypoxic-ischemic encephalopathy.** *Pediatrics* 2005;116:1001–06
50. Wijidicks EF, Campeau NG, Miller GM. **MR imaging in comatose survivors of cardiac resuscitation.** *AJNR Am J Neuroradiol* 2001;22:1561–65
51. Paulson OB, Olesen J, Christensen MS. **Restoration of autoregulation of cerebral blood flow by hypocapnia.** *Neurology* 1972;22:286–93